Quantification of Risk Factors for Osteoporosis using Thresholding Technique based on Trabecular Microarchitectures of the Proximal Femur

Ju Hwan Lee, Sung Yun Park, Jae Hoon Jeong, Sung Min Kim

Department of Medical Biotechnology, Dongguk University, 26, Pil-dong 3-ga, Jung-gu, Seoul, Korea
ykjhlee@gmail.com

Abstract: The purpose of this study was to investigate how the threshold condition used in a bone density scan influences the morphological parameters and to find an optimal threshold for predicting osteoporosis. Experimental subjects comprised a total of 54 post menopausal women aged over 40 years, who were classified into two groups, 20 normal and 34 osteoporosis patients, according to their T-scores. Bone mineral density was measured on the femoral neck, greater trochanter, and Ward's triangle by dual-energy X-ray absorptiometry. To set the threshold conditions, we employed a newly proposed thresholding method using thresholds ranging from 0 to 95% based on the trabecular bone area. We also selected seven evaluation parameters that composed of structural parameters, skeletonized parameters, and fractal dimension to evaluate the osteoporosis predictability. Based on the experimental results, we found that a threshold condition of 20% yields the most reliable predictability for osteoporosis. Quantitative evaluation also demonstrated that the statistical significances are weakened, as the threshold excessively increases.

[Lee JH, Park SY, Jeong JH, Kim SM. **Quantification of Risk Factors for Osteoporosis using Thresholding Technique based on Trabecular Microarchitectures of the Proximal Femur**. *Life Sci J* 2014;11(7):576-581] (ISSN:1097-8135). http://www.lifesciencesite.com. 79

Keywords: Osteoporosis; BMD (Bone Mineral Density); trabecular bone; DXA (Dual-energy X-ray Absorptiometry); threshold

1. Introduction

Bone mineral density (BMD) can be measured by 2D or 3D methods based on dual-energy X-ray absorptiometry (DXA) or micro computed tomography (CT), respectively [Kuroda et al., 2003]. Among these methods, micro CT systems are typically used to measure BMD mainly due to the acquisition of the various bone properties. According to the definition of the World Health Organization (WHO), osteoporosis is determined when BMD is less than or equal to 2.5 standard deviations below the young adult mean BMD [WHO, 1994]. This method, however, cannot perfectly predict the prognosis of osteoporotic fractures, and presents a different predictability for osteoporosis according to the race of the patient [Dalstra et al., 1993; Dempster et al., 1993]. This is mainly because osteoporosis is not only characterized by a low bone mass [Houam et al., 2014; Mauck and Clarke, 2006]. The aggravation of bone architecture also plays a significant role [Shi et al., 2009].

Based on these clinical characteristics, a number of morphological approaches were performed to analyze the bone architectures. The classical global method commonly separates the original image with a single threshold based on a visual measure from the gray level histogram. Hara et al. selected the optimal thresholding values for each specimen optically to separate bone structures from surrounding tissues [Hara et al., 2002]. They also evaluated how small errors in the thresholds affect the mechanical properties. Ito et al. analyzed the bone structures using manually defined threshold values from 50 to 350, and demonstrated reasonable linear correlations within the range of 100-200 [Ito et al., 1998]. Rajon et al. adopted statistical models as well as visual inspection to determine a suitable threshold [Rajon et al., 2006]. Batenburg et al. reduced the effect of the artifacts in the selection of the thresholds, and computed an optimal threshold [Batenburg and Sijbers, 2007]. On the other hand, local thresholding approaches typically apply a threshold to the original image by separating each voxel optimally within its neighborhood. Dougherty et al. successfully distinguished different degrees of osteoporosis by combining both median and local adaptive thresholding with a 7x7 window [Dougherty and Henebry, 2002]. Dufresne proposed a general local method based on the histogram of the local neighborhood voxels to compensate for the beam hardening effects [Dufresne, 1998]. Batenburg et al. suggested a local thresholding method based on projection distance minimization, and yielded accurate results [Batenburg and Sijbers, 2009].

Despite these efforts, current methods have two major limitations. First, the segmentation results are easily influenced by the original gray scale due to the threshold criteria in combination with a gradient analysis. Second, most existing approaches performed 3D analysis with micro CT. A DXA scan,

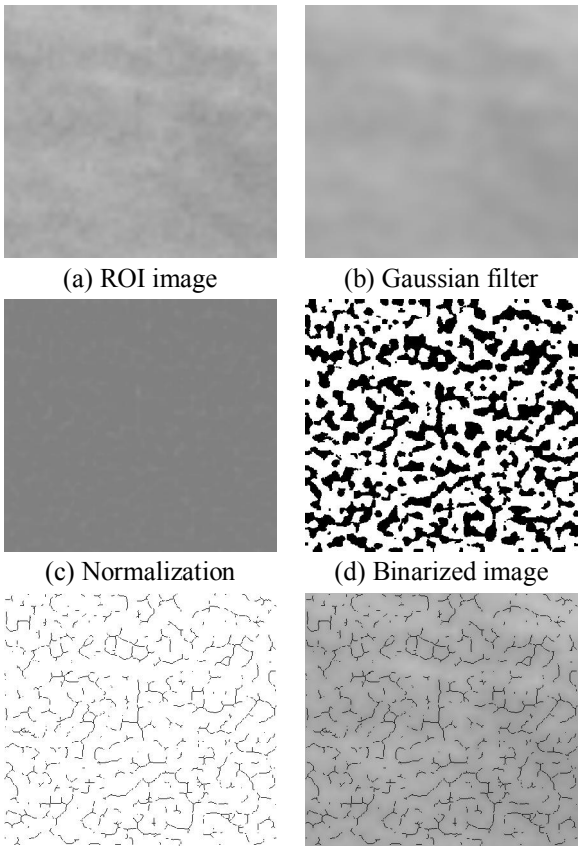

(a) ROI image (b) Gaussian filter

(c) Normalization (d) Binarized image

(e) Skeletonized image (f) Superimposed image

Figure 1. Image processing procedure for extracting the trabecular patterns from the original image

however, presents not only high spatial resolution, but also a low radiation dose and low cost compared to that of micro CT [White and Rudolph, 1999]. Therefore, if optimal threshold values that identify patients showing early signs of osteoporosis can be found on DXA scans, it will be possible to improve the predictability using a more convenient method.

The purpose of this study is to investigate how the threshold variation influences various morphological parameters and to find an optimal threshold for predicting osteoporosis on DXA radiographs. This manuscript is organized as follows. We describe the details of the overall image processing procedures for extracting trabecular microarchitectures and proposed thresholding technique in Section 2. The experimental results and its discussions are provided in Section 3 and 4, respectively. We discuss the conclusions from our findings in Section 5.

2. Material and Methods

2.1 Experimental Subjects

For our experiment, we selected a total of 54 post-menopausal women aged over 40 years who approved this study with informed consent. Subjects who suffered from a history of malignant neoplasm, surgical oophorectomy, chronical organic disorder, or femoral and spinal fracture were excluded. We also excluded subjects who had taken medication that affects bone metabolism, such as estrogen or corticosteroids. According to the standard of the WHO, experimental subjects were classified into two groups, comprising 20 normal and 34 osteoporotic patients, based on their BMD. We measured BMD on the femoral neck, greater trochanter, and Ward's triangle by using DXA with a Hologic Delphi W (Bone Densitometer, Hologic, Inc., Waltham, MA, USA).

2.2 Segmentation Procedure of the Trabecular Bone

To extract the trabecular patterns from the original DXA image, we employed a modified version of White's method [White and Rudolph, 1999]. We first identified a region of interest (ROI) in the original image (Figure 1(a)), and obtained a blurred image by using a Gaussian filter (Sigma=10

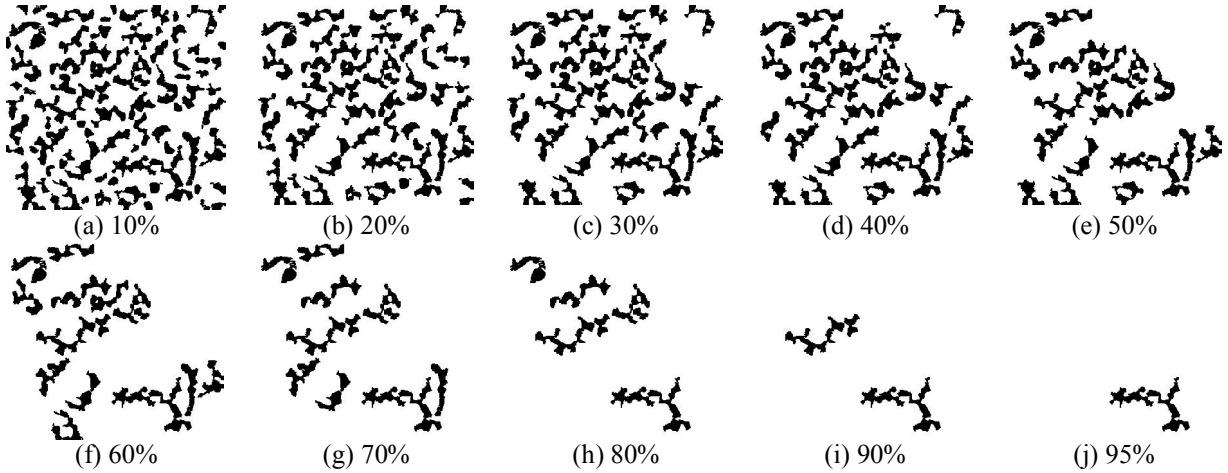

(a) 10% (b) 20% (c) 30% (d) 40% (e) 50%

(f) 60% (g) 70% (h) 80% (i) 90% (j) 95%

Figure 2. Thresholding results of the proposed method

pixels, Figure 1(b)). Next, the blurred image was subtracted from the ROI image, and 128 gray levels were added to the output image to normalize the gray scale of each pixel (Figure 1(c)). The resulting image was then binarized with a brightness value of 128 from which the trabecular bone was separated from the tissue area. We also adopted erosion and dilation operations in order to remove the shot noise, which independently appeared in the entire image (Figure 1(d)). Lastly, the skeletonized image was obtained by eroding the binary image until only the central line of pixels appeared (Figure 1(e)). We analyzed the binary and skeletonized images to extract the morphological parameters from the trabecular bone patterns. Figure 1(f) shows the superimposed image for the ROI and the skeletonized image. All image processing procedures were performed using Matlab software (R2011b, MathWorks Inc., Natick, MA).

2.3 Proposed Thresholding Technique

We propose a novel thresholding algorithm to remove the influence of the original gray levels based on the trabecular bone area. The proposed method designates the thresholding values as percentages of the trabecular bone area after dividing them into thresholds ranging from 0% to 95% based on their area (Figure 2).

The threshold percentage for each dataset can be determined by equation (1):

$$P(T) = \frac{1}{A}\int_0^{T_P} a(x)dx \qquad (1)$$

where a(x) means the area function for the trabecular bone with gray value x. T_P is the threshold value, A denotes the total area of the trabecular bone, and P represents the percentage function. After computing each trabecular area, the binarized image was segmented based on the percentages values. A certain percentage of the trabecular area was removed from the original image. In our study, we set the thresholds for the trabecular area as 0, 10, 20, 30, 40, 50, 60, 70, 80, 90 and 95%, and quantitatively evaluated the osteoporosis predictability for each threshold (Figure 2).

2.4 Evaluation Parameters

We selected seven evaluation parameters composed of four structural parameters, two skeletonized parameters, and the fractal dimension (FD) to assess the predictability for osteoporosis. The structural parameters are classified into Tb.Area, Tb.Peri, Tb.Thick and Tb.TD, and the skeletonized parameters are divided into Sk.N and Sk.Length. We computed structural parameters and FD in the binary image (Figure 1(d)), while skeletonized parameters were obtained in the skeletonized image (Figure 1(e)). Regarding the structural parameters, Tb.Area is the mean area of the total trabecular bone, and Tb.Peri is an assessment regarding the length of the trabecular perimeter. Tb.Thick shows the mean width for each trabecular bone, while Tb.TD indicates the terminal distance between the ends of adjacent bones. The skeletonized parameters, Sk.N and Sk. Length, denotes the mean number and mean length of the skeletonized elements, respectively.

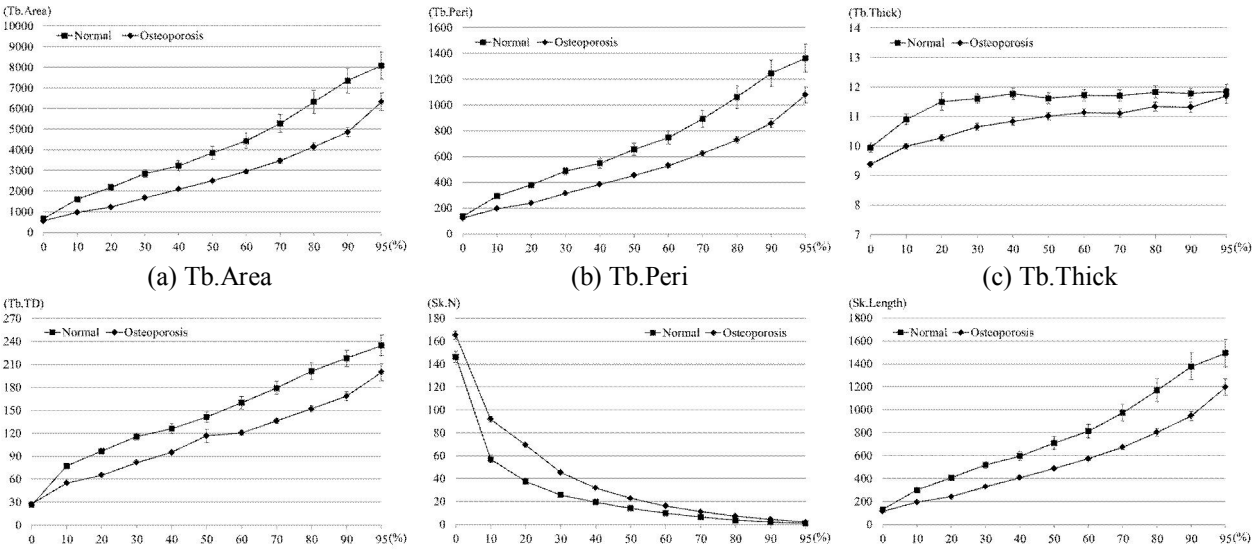

(a) Tb.Area (b) Tb.Peri (c) Tb.Thick

(d) Tb.TD (e) Sk.N (f) Sk.Length

Figure 3. Comparison of evaluation parameters between the normal and osteoporotic groups according to the different thresholding conditions (Femoral neck)

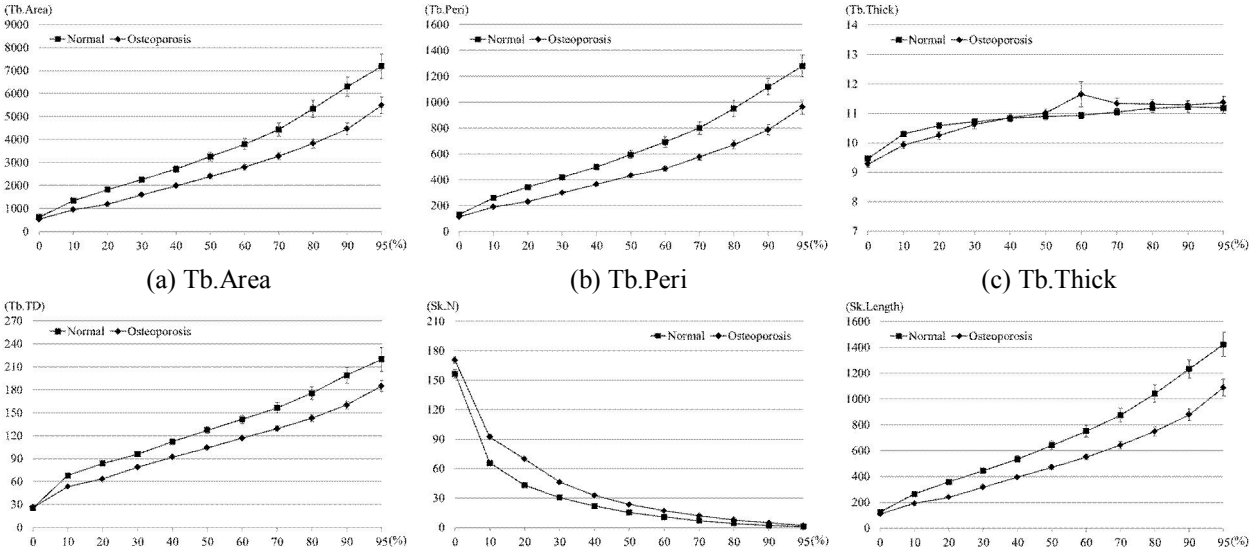

(a) Tb.Area (b) Tb.Peri (c) Tb.Thick

(d) Tb.TD (e) Sk.N (f) Sk.Length

Figure 4. Comparison of evaluation parameters between the normal and osteoporotic groups according to the different thresholding conditions (Greater trochanter)

2.5 Statistical Analysis

For statistical analyses, data were analyzed using an independent t-test based on SPSS (Ver. 12.0 for Windows, Chicago, IL, USA). A p-value of less than 0.05 was considered significant.

3. Results

In the femoral neck, all parameters, except for Tb.TD, demonstrated significant differences ($p<0.05$) between the normal and the osteoporotic groups with regards to the condition involving no thresholds, i.e., the threshold of 0% (Figure 3). The mean values of Tb.Area, Tb.Peri, Sk.N and Sk.Length showed high statistical significances for all groups, as they presented consistent variances ($p<0.05$). Tb.Thick also revealed significant differences for low threshold ranges, whereas the significance levels were deteriorated when the threshold increases (Figure 3(c)). Under the condition with no threshold (0%), Tb.TD did not significantly differ between the two groups ($p=0.617$). Increasing the thresholds, however, improved the statistical significance,

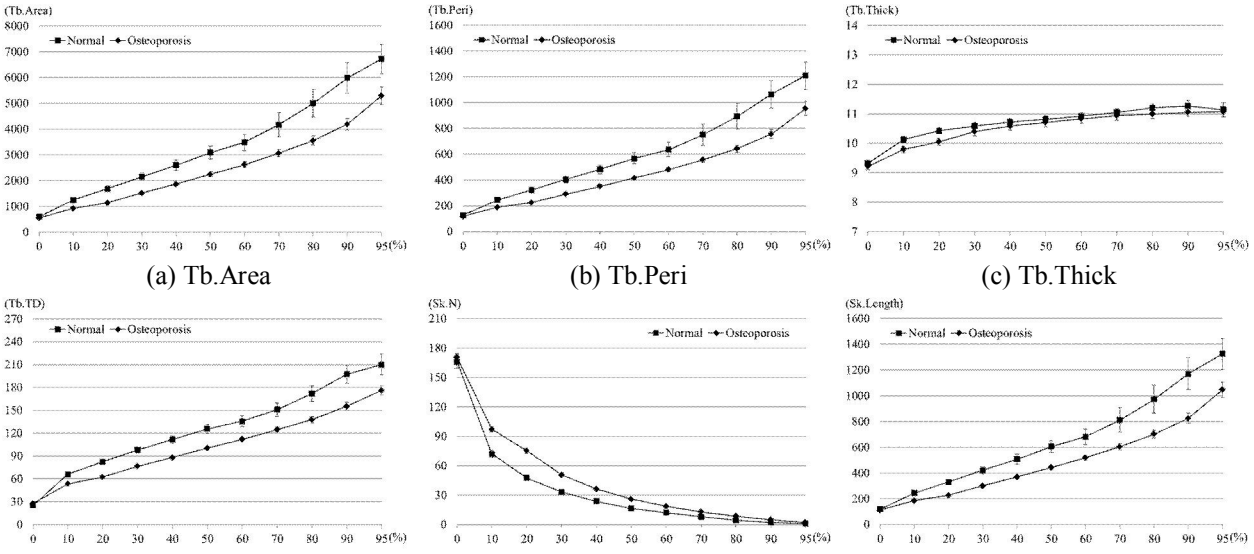

(a) Tb.Area (b) Tb.Peri (c) Tb.Thick

(d) Tb.TD (e) Sk.N (f) Sk.Length

Figure 5. Comparison of evaluation parameters between the normal and osteoporotic groups according to the different thresholding conditions (Ward's triangle)

these experimental results, we found that the

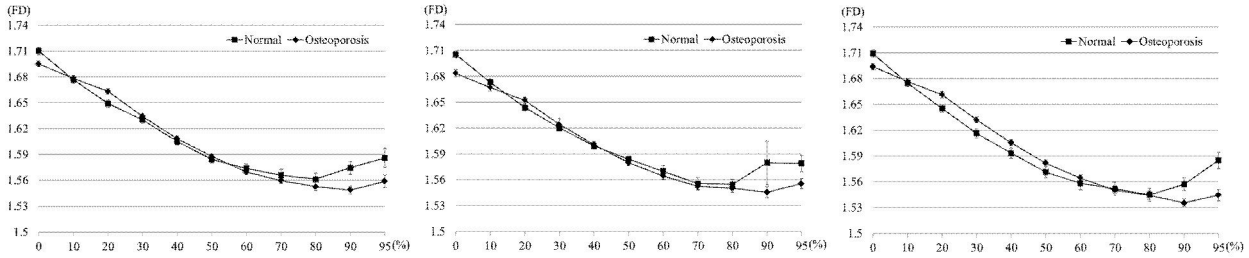

(a) Femoral neck (b) Greater trochanter (c) Ward's triangle

Figure 6. Comparison of FD between the normal and osteoporotic groups according to the different measuring regions

since the differences between the experimental groups were drastically increased (Figure 3(d)). On the other hand, FD presented significant differences only in the thresholding ranges of 0%, 20% and 90-95% (Figure 6(a)). Consequently, the threshold condition of 20% yielded the most significant differences for all experimental groups. Figure 3 compares the evaluation parameters between the experimental groups for the femoral neck.

In the greater trochanter, all parameters, except for Tb.Thick and Tb.TD, yielded high statistical significances ($p<0.05$) between the experimental groups for the condition with no thresholds (Figure 4). Tb.Thick exhibited the significant differences only in the thresholding ranges of 10-20%. When using the conditions of 60% and 70%, Tb.Thick was found to be larger in the osteoporotic group, which is dissimilar to what is observed for other conditions (Figure 4(c)). Tb.TD also did not show a significant difference for the condition with a threshold of 0% (Figure 4(d)). The statistical significance, however, was improved as the thresholds were employed. FD only revealed significant differences in the threshold conditions of 0%, 20% and 95% (Figure 6(b)). The rest of the parameters were helpful in discriminating osteoporotic patients from normal subjects, regardless of the threshold values ($p<0.05$). Figure 4 compares the parameter variances for the different thresholds on the greater trochanter.

In Ward's triangle, all parameters, except for the FD, demonstrated low significances ($p>0.05$) of differences between the experimental groups for the conditions with no thresholds (Figure 5). The significance of the differences between the normal and the osteoporotic groups, however, was continuously improved after applying the thresholds. In addition, Tb.Thick also showed significant differences between the threshold conditions of 10 and 20% (Figure 5(c)). On the other hand, the FD presented reasonable differences only in the ranges of 0%, 20-30%, and 90-95% (Figure 6(c)). Based on threshold condition of 20% reveals the highest level of significance for all parameters. It is also clear that Tb.Thick and FD provide a lower accuracy for all regions compared to the other parameters. Figure 5 compares the evaluation parameters between the normal and osteoporotic groups for Ward's triangle.

4. Discussions

Tb.Area, Tb.Peri, Tb.TD, Sk.N, and Sk.Length demonstrated relatively stable variation tendencies. Tb.Thick, however, did not show consistent variations for each condition. The differences of Tb.Thick between two groups were very small in the greater trochanter, although the significant differences were revealed within the thresholding condition of 20-30%. Tb.Thick is typically larger in the normal group than that of osteoporotic patients, since the values tend to decrease faster as BMD declines. In our experimental results, the femoral neck reflected this behavior, and Ward's triangle also allowed for significant discrimination. The greater trochanter, however, presented significant differences within narrow ranges, and significance levels were not improved as the threshold values increased. Similarly, FD also yielded an irregular tendency for each region. FD was larger in the normal group during the thresholding condition of 0% ($p<0.05$), while the threshold of 20% produced significantly opposite results ($p<0.05$). In current studies, there are numerous conflicting results as to whether FD increases [Chen and Chen, 1998] or decreases [Bollen et al., 2001] when the BMD decreases. Moreover, FD can be easily influenced by various factors due to its relatively small variances. In order to cope with these limitations, it is necessary to perform additional experiments with an extensive number of subjects. Next, in Ward's triangle, all parameters, except for FD, showed low significances for the condition with no thresholds. This result comes from the abovementioned absorptance behavior of Ward's triangle. Ward's triangle reflects more metabolic changes than other regions, whereas

the deviations for each absorptance largely differ from individual to individual. It is therefore considered that the differences of the evaluation parameters were shown to be small for the experimental groups, and the reliability for diagnosing osteoporosis was low.

5. Conclusions

The results of the present study showed that the threshold condition of 20% yields the most reliable predictability for osteoporosis. We also found that the statistical significances are weakened, as the threshold excessively increases. Based on these experimental results, we found the clinical applicability of the proposed approach for discriminating osteoporosis. A limitation of this study is that the numbers of experimental subjects are relatively small. To make the results more robust, we will analyze the trabecular patterns obtained from DXA and micro CT with more data numbers. Moreover, we will assess the predictability for osteoporotic fractures by quantifying trabecular microarchitectures.

Acknowledgements:

Foundation item: This work was supported by International Collaborative R&D Program funded by the Ministry of Knowledge Economy (MKE), Korea. (N01150049, Developing high frequency bandwidth [40-60MHz] high resolution image system and probe technology for diagnosing cardiovascular lesion)

Corresponding Author:
Dr. Sung Min Kim
Department of Medical Biotechnology
Dongguk University-Seoul
(100-715) 26, Pil-dong 3-ga, Jung-gu, Seoul, Korea
E- mail: smkim@dongguk.edu

References

1. Batenburg KJ, Sijbers J. Adaptive thresholding of tomograms by projection distance minimization. Pattern Recognit 2009;42(10):2297-2305.
2. Batenburg KJ, Sijbers J. Automatic threshold selection for tomogram segmentation by reprojection of the reconstructed image. In: Proceedings of the international conference on computer analysis of image and patterns, pp. 563-570, 2007.
3. Bollen AM, Taguchi A, Hujoel PP, Hollender LG, Fractal dimension on dental radiographs. Dentomaxillofac Radiol 2001;30(5):270-275.
4. Chen SK, Chen CM. The effects of projection geometry and trabecular texture on estimated fractal dimensions in two alveolar bone models. Dentomaxillofac Radiol 1998;27(5):270-274.
5. Dalstra M, Huiskes R, Odgaard A, van Erning L. Mechanical and textural properties of pelvic trabecular bone. J Biomech 1993;26(4-5):523-535.
6. Dempster DW, Ferguson-Pell MW, Mellish RW, Cochran GV, Xie F, Fey C, Horbert W, Parisien M, Lindsay R. Relationships between bone structure in the iliac crest and bone structure and strength in the lumbar spine. Osteoporosis Int 1993;3(2):90-96.
7. Dougherty G, Henebry GM. Lacunarity analysis of spatial pattern in CT images of vertebral trabecular bone for assessing osteoporosis. Med Eng Phys 2002;24(2):129-138.
8. Dufresne T. Segmentation techniques for analysis of bone by three-dimensional computed tomographic imaging. Technol Health Care 1998;6(5-6):351-359.
9. Hara T, Tanck E, Homminga J, Huiskes R. The influence of microcomputed tomography threshold variations on the assessment of structural and mechanical trabecular bone properties. Bone 2002;31(1):107-109.
10. Houam L, Hafiane A, Boukrouche A, Lespessailles E, Jennane R. One dimensional local binary pattern for bone texture characterization. Pattern Anal Applic 2014;17(1):179-193.
11. Ito M, Nakamura T, Matsumoto T, Tsurusaki K, Hayashi K. Analysis of trabecular microarchitecture of human iliac bone using microcomputed tomography in patients with hip arthrosis with or without vertebral fracture. Bone 1998;23(2):163-169.
12. Kuroda S, Mukohyama H, Kondo H, Aoki K, Ohyma T, Kasugai S. Bone mineral density of the mandible in ovariectomized rats: analyses using dual energy X-ray absorptiometry and peripheral quantitative computed tomography. Oral Dis 2003;9(1):24-28.
13. Mauck KF, Clarke BL. Diagnosis, screening, prevention, and treatment of osteoporosis. Mayo Clin Proc 2006;81(5):662-672.
14. Rajon DA, Pichardo JC, Brindle JM, Kielar KN, Jokisch DW, Patton PW, Bolch WE. Image segmentation of trabecular spongiosa by visual inspection of the gradient magnitude. Phys Med Biol 2006;51(18):4447-4467.
15. Shi X, Wang X, Niebur GL. Effects of loading orientation on the morphology of the predicted yielded regions in trabecular bone. Ann Biomed Eng 2009;37(2):354-362.
16. White SC, Rudolph DJ. Alterations of the trabecular pattern of the jaws in patients with osteoporosis. Oral Surg Oral Med Oral Pathol Oral Radiol Endod 1999;88(5):628-635.
17. WHO. Assessment of fracture risk and its application to screening for postmenopausal osteoporosis, WHO Technical report Series. Geneva 1994.

5/26/2014